CHIN. PHYS. LETT. Vol. 36, No. 1 (2019) 014203

Asymmetric and Single-Side Splitting of Dissipative Solitons in Complex Ginzburg–Landau Equations with an Asymmetric Wedge-Shaped Potential *

Yun-Cheng Liao(廖云程)[1], Bin Liu(刘彬)[1**], Juan Liu(刘娟)[1], Jia Chen(陈佳)[2]

[1]*National Engineering Laboratory for Destructive Testing and Optoelectronic Sensing Technology and Application, Nanchang HangKong University, Nanchang 330063*

[2]*Nanchang Institute of Science and Technology, Nanchang 3301608*

(Received 17 September 2018)

We report some novel dynamical phenomena of dissipative solitons supported by introducing an asymmetric wedge-shaped potential (just as a sharp 'razor') into the complex Ginzburg–Landau equation with the cubic-quintic nonlinearity. The potentials corresponding to a local refractive index modulation with breaking symmetry can be realized in an active optical medium with respective expanding antiwaveguiding structures. Using the razor potential acting on a central dissipative soliton, possible outcomes of asymmetric and single-side splitting of dissipative solitons are achieved with setting different strengths and steepness of the potentials. The results can potentially be used to design a multi-route splitter for light beams.

PACS: 42.65.Tg, 05.45.−a DOI: 10.1088/0256-307X/36/1/014203

The complex Ginzburg–Landau (CGL) equation is an important model which occurs in many areas, such as superconductivity and superfluidity, fluid dynamics, reaction diffusion phenomena, nonlinear optics, Bose–Einstein condensates, and quantum field theories.[1,2] Dissipative soliton (DS) is an important class of patterns observed and reproduced in these media by the CGL equations.[3,4] In 1984, Petviashvili and Sergeev firstly proposed the CGL equation with the cubic-quintic nonlinearity as a model generating stable localized modes.[5] Then, the CGL equation with the cubic-quintic nonlinearity has been widely used in nonlinear dissipative optics, due to the clear physical meaning of all its terms in any particular application, such as passively mode-locked laser systems and optical transmission lines.[6] Some typical nonlinear optical media that feature the cubic-quintic response include chalcogenide glasses[7] and some organic materials.[8] Subsequently, numerous complex stable patterns and novel dissipative dynamics in this model have been investigated, including stable dissipative vortices,[9] DS clusters,[10−12] necklace-ring patterns,[13,14] bound states,[15] dissipative optical bullets,[16] phase controlling of DSs collision,[17−19] and self-structuring of breathing vortices.[20] In recent years, a series of novel dynamics of DSs have been reported by adding refractive-index modulation as an external potentials in CGL models such as continuous splitting of DSs and concentric waves expanding.[21−23]

In this Letter, we introduce the one-dimensional cubic-quintic CGL equation with an asymmetric wedge-shaped potential (AWSP). We consider the action of these potentials on a stable DS initially placed at the central position (apex of the potential). The AWSP, just like a 'razor' with two sides of different sharpness, is used to cut the central soliton. The dynamical phenomena of asymmetrical and single-side splitting of DS streams from the central DS are numerically investigated in detail.

We consider the one-dimensional cubic-quintic CGL equation in the general form which describes the evolution equation for the amplitude of the electromagnetic wave in an active bulk optical medium,[15]

$$iu_z + i\delta \cdot u + (1/2 - i\beta)u_{xx+(1-i\varepsilon)|u|^2u} - (\nu - i\mu)|u|^4u = V(x)u, \tag{1}$$

where z and x are the propagation distance and transverse coordinate, respectively. The coefficients of the diffraction and cubic self-focusing nonlinearity are scaled, respectively, to be $1/2$ and 1, while $\nu < 0$ accounts for the quintic self-defocusing, δ is the coefficient corresponding to linear loss ($\delta > 0$) or gain ($\delta < 0$), $\mu > 0$ is the quintic-loss parameter, $\varepsilon > 0$ the cubic-gain coefficient, and $\beta > 0$ accounts for an effective diffusion (viscosity). Generic results may be adequately represented by setting $\delta = 0.5$, $\mu = 1$, $\varepsilon = 2$, $\beta = 0.5$, and $\nu = 0.115$ in Eq. (1). The last term on the right-hand side of Eq. (1) introduces an AWSP in the transverse plane, $V(x)$, which depends on the x coordinate,

$$V(x) = \begin{cases} -a_1|x|^{n_1}, & x \geqslant 0, \\ -a_2|x|^{n_2}, & x < 0, \end{cases} \tag{2}$$

where a_1 and a_2 indicate the strengths of potentials, n_1 and n_2 are the steepness of potentials.

*Supported by the National Natural Science Foundation of China under Grant No 61665007, and the Natural Science Foundation of Jiangxi Province under Grant No 20161BAB202039.

**Corresponding author. Email: liubin_d@126.com

© 2019 Chinese Physical Society and IOP Publishing Ltd

The desirable patterns of the refractive-index modulation in materials described by the CGL equation, which may induce the effective potentials, can be achieved by means of various techniques, such as optics induction[24] and writing patterns by streams of ultrashort laser pulses.[25] The initial state is a stable DS solution of the cubic-quintic CGL equation without potential. The stable DS places at the apex of the wedge-shaped potential ($x = 0$). We use the following isotropic ansatz for DS solution in the general case[15]

$$u = A(z) \exp\Big[-\frac{x^2}{2w^2(z)} + ic(z)x^2 + i\phi(z) \Big], \quad (3)$$

where A, w, c and ϕ represent the amplitude, width, wavefront curvature, and overall phase, respectively. If $a_1 = a_2$ and $n_1 = n_2$, $V(x)$ degenerates into a symmetric wedge-shaped potential representing anti-waveguiding structures in the optical medium. Some typical dynamic characteristics have been studied and novel continuous splitting phenomena of dissipative solitons have been revealed.[21–23] The viscosity term in Eq. (1), $\sim \beta$, plays an important role in maintaining the position of a central soliton. With slight or zero viscosity, the central soliton is always subject to the drift instability, starting to roll down from the tip of the potential.

First, we consider the AWSP with linear slopes along $\pm x$ by setting $n_1 = n_2 = 1$. In Fig. 1(a), the dashed line represents a typical curve of AWSP with $a_1 \neq a_2$, and the solid line indicates the initial DS placed at the top of AWSPs. Then, simulations of Eq. (1) reveal a series of novel dynamical phenomenon, obtained by varying a_1 and a_2 in the range of 0.19–0.4. We can observe continuous splitting of DS streams from the initial soliton. For $a_1 = a_2$, the soliton streams which continuously split from two sides of the initial soliton are perfectly symmetric (shown in Fig. 1(b)). The gain term in the cubic-quintic CGL equation is the energy source necessary for this dynamical phenomenon.

Then, for an asymmetric slope ($a_1 \neq a_2$), the applied force of the potential on the initial soliton also becomes of unbalance. However, for $0.19 \leqslant a_1 \neq a_2 \leqslant 0.4$, the initial soliton can also stay in the center and continuously split DS streams. A typical sample of this dynamical evolution is simulated in Fig. 1(c) with $a_1 = 0.22$ and $a_2 = 0.31$. However, an obvious different splitting rate can be observed along $\pm x$. The stronger potential can provide a higher splitting rate, thus the DS streams on the right are obviously less than those on the left.

Nevertheless, if one or both of a_1 and a_2 are less than 0.19, no matter how small the gap is between a_1 and a_2, the initial soliton cannot keep in the center and will slide towards more steep side, as shown in Fig. 1(d).

Assuming $a_2 > 0.4$ and $0.19 \leqslant a_1 \leqslant 0.4$, the left potential's slope will exceed the critical value admitting steady motion of the DSs.[24] Although the initial soliton survives, despite the fact that it sits on the potential maximum. However, the splintered pulses rapidly dissipate, failing to self-trap into secondary DS streams. As shown in Fig. 1(e), when $a_2 = 0.45$, the DS streams on the left-hand side of the initial soliton cannot be generated. Thus the phenomena of continuous splitting DSs only occur on the right-hand side.

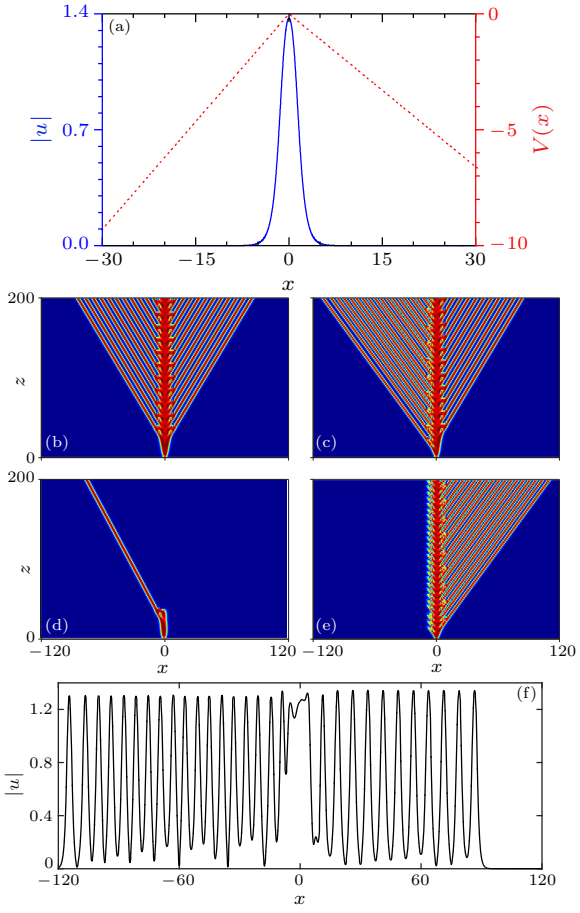

Fig. 1. (Color online) Dynamics of DSs on top of the AWSP with $n_1 = n_2 = 1$. (a) The profile of the initial soliton (solid curve) and the shape of the AWSP with $a_1 = 0.22$ and $a_2 = 0.31$ (dashed curve). (b)–(e) Isosurface plots of total intensity $|u(x)|^2$, evolutions of the initial soliton with ($a_1 = a_2 = 0.22$), ($a_1 = 0.22$ and $a_2 = 0.31$), ($a_1 = 0.18$ and $a_2 = 0.19$), and ($a_1 = 0.31$ and $a_2 = 0.45$), respectively. (f) The transverse profile of the output beam corresponding to (c).

Next, we further study the dynamical characteristics with nonlinear slopes by setting potential steepness $n_1 = n_2 = 0.5$. As shown in Fig. 2(a), the solid and dashed lines represent a typical AWSP with $a_1 \neq a_2$ and the initial soliton, respectively. For $0.5 \leqslant a_1 \neq a_2 \leqslant 0.94$, an asymmetrical continuous splitting of DSs are observed, A typical example is

shown in Fig. 2(b) with $a_1 = 0.7$ and $a_2 = 0.9$. Due to $a_1 < a_2$, a higher splitting rate can be obtained on the left-hand side. However, because of steepness of potentials $n_1 = n_2 = 0.5 < 1$, the slopes gradually become lower. Thus the gap between DSs also decreases gradually. This leads to the merger of the DSs because of the strong interaction between them, just as in the phenomena A and B shown in Fig. 2(b). When only a_1 exceeds 0.94, the initial soliton will completely split into two parts (shown in Fig. 2(c)). However, if a_1 or $a_2 > 1.5$, the corresponding splitting part will rapidly dissipate, as shown in Fig. 2(e). In addition, assuming $0.32 \leqslant a_1 < 0.5$ and $0.5 \leqslant a_2 \leqslant 0.94$, the DS streams are not split from the right-hand side of the initial solitons. The dynamical phenomenon of single-side continuous splitting can be observed in Fig. 2(d).

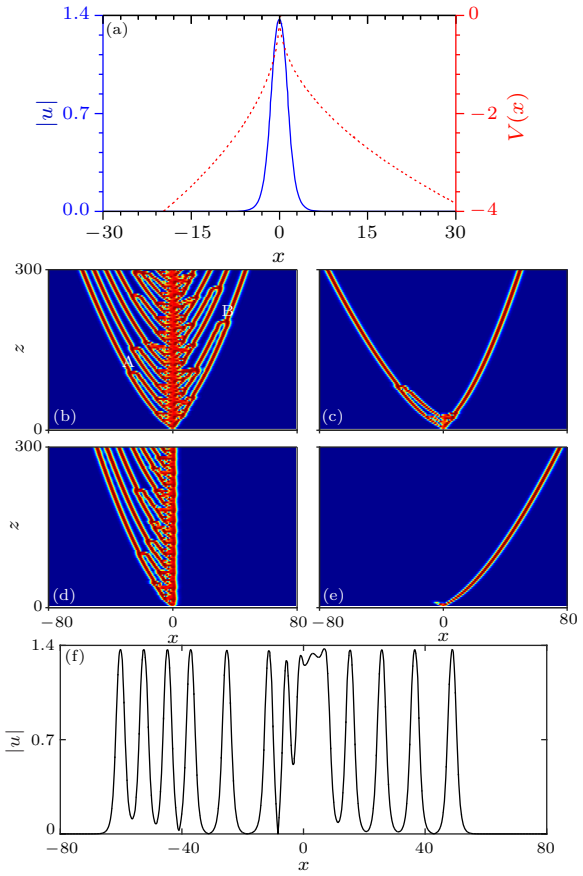

Fig. 2. Dynamics of DSs on top of the AWSP with $n_1 = n_2 = 0.5$. (a) The profile of the initial soliton (solid curve) and the shape of the AWSP with $a_1 = 0.7$ and $a_2 = 0.9$ (dashed curve). (Color online) (b)–(e) For $n_1 = n_2 = 0.5$, isosurface plots of total intensity $|u(x)|^2$, evolutions of the initial soliton with ($a_1 = 0.7$, $a_2 = 0.9$), ($a_1 = 0.7$, $a_2 = 1.3$), ($a_1 = 0.4$, $a_2 = 0.7$), and ($a_1 = 1.3$, $a_2 = 1.7$), respectively. (f) The transverse profile of the output beam corresponding to (b).

Finally, we systematically study the dynamics of asymmetric splitting of DSs with $n_1 \neq n_2$ and $a_1 \neq a_2$. With values of n_1 and n_2 from 0.3 to 1.1, there are corresponding ranges of a_1 and a_2 for the dynamics of asymmetric splitting of DSs. By performing much numerical simulations, the dynamics regions of a_1 and a_2 for different n_1 and n_2 are plotted as the floating columns in Fig. 3(a). In other words, as long as the modulation parameter (a_1 and n_1) of the potential along $+x$ and (a_2 and n_2) along $-x$ is taken in this region of the floating columns, we can obtain the corresponding dynamics of continuous splitting. Figures 3(b) and 3(c) shows two samples of dynamical evolutions of asymmetric splitting with ($n_1 = 1$, $a_1 = 0.2$, $n_2 = 0.5$, $a_2 = 0.7$) and ($n_1 = 0.4$, $a_1 = 0.9$, $n_2 = 0.8$, $a_2 = 0.4$).

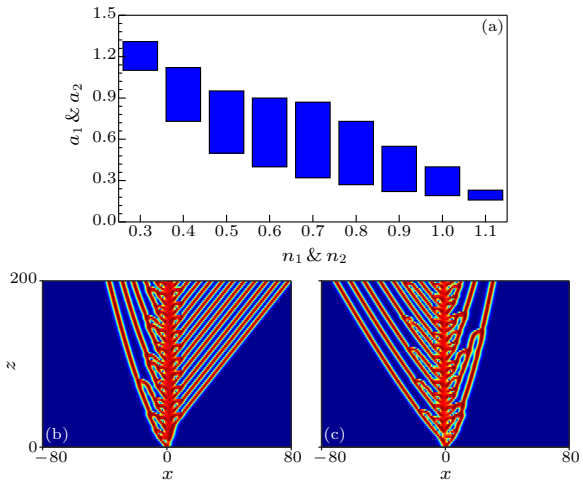

Fig. 3. (Color online) (a) The dynamics regions of asymmetric splitting of DSs in the plane of (a_1 and a_2, n_1 and n_2). (b), (c) Isosurface plots of total intensity $|u(x)|^2$, evolutions of the initial soliton with ($n_1 = 1$, $a_1 = 0.2$, $n_2 = 0.5$, $a_2 = 0.7$) and ($n_1 = 0.4$, $a_1 = 0.9$, $n_2 = 0.8$, $a_2 = 0.4$).

In summary, we have introduced an AWSP in the form of a sharp 'razor' into a one-dimensional CGL equation with the cubic-quintic nonlinearity. By placing the initial soliton at the apex of the asymmetric razor, we observe the asymmetric and single-side splitting of DSs, rolling down of the whole soliton along the potential slope. The dynamic status of each side can be independently controlled with the corresponding parameter (n_1, a_1) or (n_2, a_2) of the potential within limits. These results can extend the analysis to the higher-dimensional version of the CGL model and can provide potential applications to the design of all-optical data processing schemes.

References

[1] Aranson I S and Kramer L 2002 *Rev. Mod. Phys.* **74** 99
[2] Malomed B A 2005 *Encyclopedia Nonlinear Sci.* p 157
[3] Bakonyi Z, Michaelis D et al 2002 *J. Opt. Soc. Am. B* **19** 487
[4] Ultanir E A, Stegeman G I et al 2003 *Phys. Rev. Lett.* **90** 253903
[5] Petviashvili V I and Sergeev A M 1984 *Dokl. Akad. Nauk SSSR* **276** 1380
[6] Akhmediev N N, Ankiewicz A et al 1998 *J. Opt. Soc. Am. B* **15** 515

[7] Boudebs G, Cherukulappurath S et al 2003 *Opt. Commun.* **219** 427
[8] Zhan C, Zhu D, Li D et al 2002 *J. Opt. Soc. Am. B* **19** 369
[9] Mihalache D, Mazilu D, Lederer F et al 2006 *Phys. Rev. Lett.* **97** 073904
[10] Vladimirov A G, McSloy J M, Skryabin D V et al 2002 *Phys. Rev. E* **65** 046606
[11] Skryabin D V and Vladimirov A G 2002 *Phys. Rev. Lett.* **89** 044101
[12] Li H, Lai S, Qui Y et al 2017 *Opt. Express* **25** 27948
[13] He Y J, Wang H Z and Malomed B A 2007 *Opt. Express* **15** 17502
[14] Liu B, He Y J, Qiu Z R et al 2009 *Opt. Express* **17** 12203
[15] He Y J, Malomed B A, Mihalache D et al 2009 *Opt. Lett.* **34** 2976
[16] Djoko M and Kofane T C 2017 *Commun. Nonlinear Sci. & Numer. Simul.* **48** 179
[17] Mihalache D, Mazilu D, Lederer F et al 2009 *Eur. Phys. J. Spec. Top.* **173** 245
[18] Liu B, He X D and Li S J 2011 *Phys. Rev. E* **84** 056607
[19] Liu B, Liu Y F and He X D 2014 *Opt. Express* **22** 26203
[20] Skarka V, Aleksić N B et al 2017 *Opt. Express* **25** 10090
[21] He Y J, Malomed B A, Ye F et al 2010 *J. Opt. Soc. Am. B* **27** 1139
[22] Liu B and He X D 2011 *Opt. Express* **19** 20009
[23] Liu B, He X D and Li S J 2013 *Opt. Express* **21** 5561
[24] Cleff C, Gütlich B and Denz C 2008 *Phys. Rev. Lett.* **100** 233902
[25] Szameit A, Burghoff J et al 2006 *Opt. Express* **14** 6055